SLAC–PUB–7862 (Revised)
November 1998

Calculations of the Short-Range Longitudinal Wakefields in the NLC Linac*

K.L.F. Bane
Stanford Linear Accelerator Center, Stanford University, Stanford, CA 94309
A. Mosnier
CEA Saclay, Gif-sur-Yvette Cedex, France
A. Novokhatskii
Technische Hochschule Darmstadt, Darmstadt, Germany
K. Yokoya
KEK High-Energy Physics Laboratory, Tsukuba, Japan

Abstract

Using two frequency domain and one time domain numerical approaches, we calculate the short-range longitudinal wakefield of the NLC linac accelerating structure, and find that the results agree to $\sim 5\%$. We show that our results are consistent with an analytical formula for the impedance at high frequencies. We, in addition, obtain through fitting a simple formula for the short-range wakefield of a linac structure that can be useful in designing linear colliders. Finally, we demonstrate that for the NLC linac cavity the effects on the short-range wake of end conditions, tapering, and rounding of the irises are small.

Presented at ICAP '98
Monterrey, CA
September 14–18, 1998

*Work supported by Department of Energy contract DE–AC03–76SF00515.

CALCULATIONS OF THE SHORT-RANGE LONGITUDINAL WAKEFIELDS IN THE NLC LINAC

K.L.F. Bane, SLAC, Stanford, USA; A. Mosnier, Saclay, France;
A. Novokhatski, TH Darmstadt, Germany; K. Yokoya, KEK, Tsukuba, Japan

Abstract

Using two frequency domain and one time domain numerical approaches, we calculate the short-range longitudinal wakefield of the NLC linac accelerating structure, and find that the results agree to $\sim 5\%$. We show that our results are consistent with an analytical formula for the impedance at high frequencies. We, in addition, obtain through fitting a simple formula for the short-range wakefield of a linac structure that can be useful in designing linear colliders. Finally, we demonstrate that for the NLC linac cavity the effects on the short-range wake of end conditions, tapering, and rounding of the irises are small.

1 INTRODUCTION

In the Next Linear Collider (NLC)[1] trains of short, intense bunches are accelerated through the linac on their way to the collision point. In the linac the transverse modes of the accelerating cavities will be damped and detuned to control long-range wakefield effects. The dominant, remaining current-dependent effects will be those due to the short-range wakefields. A calculation of short-range wakefields in the NLC linac structure has been given in Ref. [2]. However, due to the difficulty in obtaining these functions accurately to the very short distances required—or equivalently, the impedances to the very high frequencies required—we revisit in this report the earlier results, and compare them with those of other calculation methods.

For our purposes an accelerating cavity of the NLC linac can be modeled by a periodic structure. For a periodic structure at high frequencies, the real part of the longitudinal impedance varies as $\omega^{-3/2}$ and the imaginary part as ω^{-1}[3, 4, 5]; correspondingly, the wakefield at the origin $W_L(0) = Z_0 c/(\pi a^2)$[5], with $Z_0 = 377\ \Omega$ and a the iris radius, and for short distances s, $W_L'(s) \sim s^{-1/2}$. To obtain the short range wakefields of a periodic structure, according to the method used in Ref. [2] (see also[6]), the impedance is first obtained over a finite frequency range through field matching. The high frequency portion is taken to be given by the so-called Sessler-Vaynstein optical resonator model[3], a model that asymptotically satisfies the appropriate power law. The resulting function is then Fourier transformed to obtain the short-range wakefield.

In this report a second method[7] will be applied to the problem, one that uses a similar approach, though with the impedance calculated along a path slightly shifted from the real frequency axis. This impedance function is much smoother: it is easier to study its asymptotic behavior and easier to Fourier transform. A third method[8], one that uses direct, time domain integration to obtain the wakefield is also applied. This method has the advantage of being able to find wakes of non-periodic structures. We will, in addition, compare the numerical results to a high-frequency analytical formula due to Gluckstern[5]. Note that we designate the three numerical methods as, respectively, the frequency domain (FD), the complex frequency domain (CFD), and the time domain (TD) approach.

In this report we will also perform parameter studies for a periodic structure, to obtain a simple formula for the wake that may be useful in designing a linear collider. Finally, again using the example of the NLC linac cavity, we study the effects of the rounding of the irises, and the effects of non-periodic features, such as the variation in cell geometry, and the end conditions.

2 FREQUENCY DOMAIN METHODS

The NLC accelerating cavity is a 206 cell damped, detuned structure (DDS) operating at 11.4 GHz. It is a disk-loaded structure, with constant period L ($= 8.75$ mm), and gradually varying gap g and minimum iris radius a (the iris edges are rounded). In the version named DDS1, for example, the change in a follows a Gaussian distribution with rms 2.5%, truncated at $\pm 2\sigma$, and g varies from 7.75 mm to 6.75 mm. The middle cell has dimensions $a = 4.724$ mm and $g = 7.25$ mm. Note that since the NLC linac bunch length is very small (with rms $\sigma_z = 0.1$ mm), the bunch "sees" only the irises, and the outer cavity shape plays no role in the wakefield. Let us begin by considering a purely periodic model of an NLC cavity. We choose the same model as was used in Ref. [2], *i.e.* one with squared, not rounded, iris edges, and with dimensions $a = 4.924$ mm, $g = 6.89$ mm, and $L = 8.75$ mm.

According to the FD method, the wave numbers k_n and the loss factors κ_n for a few hundred modes are obtained by field matching, and the high frequency dependence of the impedance is given by the optical resonator model. The real part of the impedance becomes

$$R_L = \sum_{n=1}^{N} \frac{\pi\kappa_n}{c}\delta(k-k_n) + \frac{2Z_0 j_{01}^2}{\pi L\zeta^2} \times \times \frac{\sqrt{\nu}+1}{(\nu+2\sqrt{\nu}+2)^2}\Theta(k-k_N) \quad k>0 \quad , \tag{1}$$

with $j_{01} = 2.41$, $\zeta = 0.824$, $\nu = 4a^2k/(\bar{L}\zeta^2)$, with c the speed of light and $\bar{L} = \sqrt{Lg}$; $\Theta(x) = 0$ for $x < 0$, 1 for $x > 0$. The resonator model combines the power spectrum at the iris edge in the primary field of the beam with diffraction at the edges of a periodic array of thin, circular mirrors. It is a simple model but it has been observed to agree well with numerical results. The real part of the impedance of our model as obtained by the FD method, with 270 modes averaged over frequency bins, is given by the histogram in Fig. 1. The optical resonator asymptote is given by a dotted curve. We see that at higher frequencies the two agree.

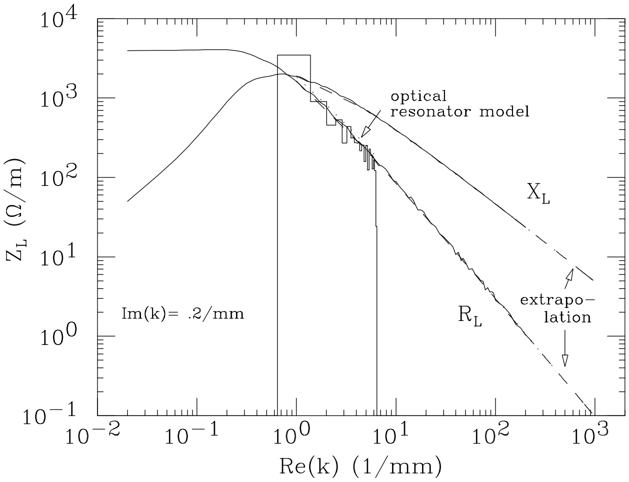

Figure 1: R_L, when averaged over bins, as given by the FD method (histogram); R_L and X_L as given by the CFD method (solid lines) and by Eq. 2 with $\alpha = 0.52$ (dashes).

The CFD method also finds the impedance by field matching, but along a path slightly shifted off the real k axis. In Fig. 1 the real (R_L) and imaginary (X_L) parts of the impedance Z_L, as obtained by this method, when $k_I = \mathrm{Im}(k) = 0.2$ mm^{-1}, are shown (the solid curves). We note that the impedance is a relatively smooth function (instead of a sum of delta functions as before), and that the results agree well with those of the FD method and with the optical resonator model. Note that with the CFD method we can accurately go to much higher frequencies than before, and can therefore better study the asymptotic behavior of the impedance. For example, with the FT method, since the density of modes varies $\sim k$, we would need to solve for 3×10^5 modes to obtain Z_L up to $k = 200$ mm^{-1}. We should point out, however, that even with the CFT method to get convergence in the solution at high frequencies, the size of the matrix we need to solve becomes very large: at $k_R = 200$ mm^{-1} its size is $\sim 600 \times 600$.

Gluckstern gives the high frequency behavior of the impedance of a periodic structure as[5]:

$$Z_L \approx \frac{iZ_0}{\pi k a^2}\left[1 + (1+i)\frac{\alpha L}{a}\left(\frac{\pi}{kg}\right)^{1/2}\right]^{-1} \qquad [k \text{ large}] \, , \tag{2}$$

with the parameter $\alpha = 1$. It can be shown, however, that α is a function of g/L, with $\alpha(0) = 1$ and $\alpha(1) = 0.46$[9]. (Note that 0.46 is the same numerical factor that has been obtained by Stupakov for a periodic array of infinitesimally thin irises[10].) For normal structures ($g/L \approx 1$), $\alpha \approx 0.5$. Eq. 2 with the appropriate α for our dimensions, 0.52, is shown in Fig. 1 by the two dashed curves. We note good agreement with the CFD results at high frequencies.

2.1 *Longitudinal Wakefield*

In the FD method the short-range longitudinal wakefield $W_L(s)$ is obtained by inverse Fourier transforming the impedance. The same is true in the CFD method, except that the result must also be multiplied by the factor $\exp(k_I s)$. The results are shown in Fig. 2. There is about a 5% disagreement between the two results. One check is that $W_L(0)$ should equal $Z_0/(\pi a^2)$. The result of the FD method is 6% low, that of the CFD method is 1% low.

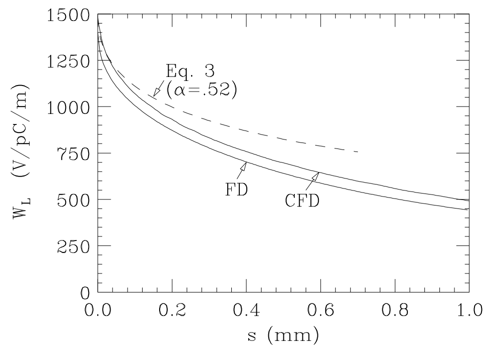

Figure 2: The wakefield of our periodic model, as obtained by different frequency domain methods.

If we inverse Fourier transform Eq. 2 we obtain a prediction for the very short-range wakefield:

$$W_L \approx \frac{Z_0 c}{\pi a^2}\exp\left(\frac{2\pi\alpha^2 L^2 s}{a^2 g}\right)\mathrm{erfc}\left(\frac{\alpha L}{a}\sqrt{\frac{2\pi s}{g}}\right) \quad [s\,\mathrm{small}] \tag{3}$$

(given by the dashes in Fig. 2). We see that the approximate result, Eq. 3, agrees well with the CFD result for very short distances, for $s \lesssim 50\ \mu$m.

2.2 *Parameter Study*

For designing linear colliders it would be useful to have a simple approximate formula for the short-range wakefield of a periodic structure that is valid, say, up to $s/L = .15$ ($s = 1.3$ mm for the NLC), over possible values of a and g. For this purpose we repeat the CFD calculation for parameters in the region $.34 \leq a/L \leq .69$ and $.54 \leq g/L \leq .89$. Anticipating the functional form

$$W_L = \frac{Z_0 c}{\pi a^2}\exp\left(-\sqrt{s/s_0}\right) \quad , \tag{4}$$

we plot in the left frame of Fig. 3 the values of s_0 fitted to the numerical results (the plotting symbols). We find the data is reasonably well reproduced by taking

$$s_0 = 0.41\frac{a^{1.8}g^{1.6}}{L^{2.4}} \tag{5}$$

(the dashes in the figure). In the right frame we plot the wakes and the model result for four examples at the corners of our parameter plane. Note that a similar, though different, wakefield model has been proposed in Ref. [11].

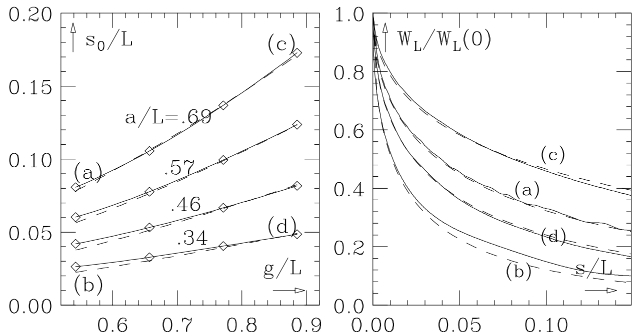

Figure 3: Results of our parameter study.

3 TIME DOMAIN CALCULATIONS

The TD method that we employ uses direct time domain integration of Maxwell's equations to obtain the wakefield. It uses an implicit method to solve finite difference equations, taking care to avoid dispersive errors that tend to occur in mesh-based programs at high frequencies. The program finds the wake of a bunch distribution (typically a Gaussian), $\bar{W}_L$. It has been used successfully for cases with extremely small bunch lengths, such as in TESLA-FEL, where $\sigma_z/a \sim 10^{-3}$[8]. The bunch wake is connected to W_L through

$$\bar{W}_L(s) = -\int_0^\infty W_L(s')\lambda(s-s')\,ds' \quad , \qquad (6)$$

with $\lambda(s)$ the charge distribution. In our simulations we will use the nominal NLC bunch length, $\sigma_z = 0.1$ mm.

First, for our periodic example we let the bunch continue through identical cells until the wake per cell no longer changes. The result of the TD simulation is given in Fig. 4, and compared with that of the CFD method, after it has been convolved according to Eq. 6 (the dashes). The results are almost identical. When comparing total loss factors κ_{tot} the results for the TD, CFD, and FD methods are, respectively, 545, 547, and 512 V/pC/m.

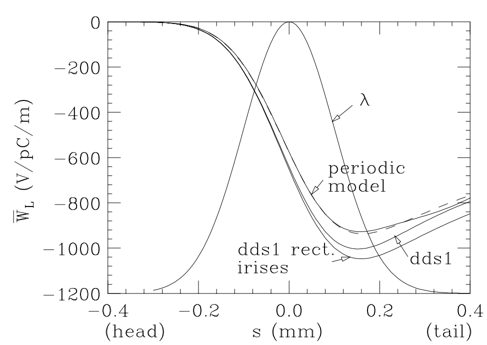

Figure 4: Results of the time domain (TD) calculations.

Features of the DDS1 cavity that are not in our periodic model are transients at the beginning of the cavity, the tapering of the cell geometry in the cavity, and the rounding of the iris edges, the effects of which we can explore with the TD method. As to the transients, it can be shown[4, 5, 12] that for a finite number of cells greater than a certain critical number $N_{crit} \gtrsim a^2/(2L\sigma_z)$ the average wake per cell of the finite structure agrees to within a few percent with that of the periodic structure. In our case this corresponds to only 14 cells (out of 206), so this should not be a significant effect. We can also estimate the effect of the tapering on the wakefield. For example, let us consider the effect on κ_{tot}, which for the short NLC bunch scales $\sim a^{-2}$. If we integrate this scaling over the Gaussian distribution in a, we find that over a whole cavity (assuming we can ignore the transients) $\langle\kappa_{tot}\rangle = \kappa_{tot}(\bar{a})(1+\sigma^2)$, with $\bar{a}$ the average iris radius and σ the rms of the distribution in a ($= 2.5\%$). That is, the expected result is nearly the same as for a periodic structure with dimension $a = \bar{a}$.

We have performed a TD calculation for an entire, tapered DDS1 cavity, once with squared irises and once with the actual (rounded) iris shapes (see Fig. 4). Comparing loss factors, we obtain, for the squared irises, $\kappa_{tot} = 617$ V/pC/m, which is 13% larger than for the periodic model. However, remember that in the periodic model $a = 4.924$ mm, which is 4% larger than $\bar{a}$ in the actual structure, so considering the a^{-2} scaling of the wakefield there is only a 5% discrepancy unaccounted for, which could be due to the end conditions and/or the tapering. Finally, for the actual DDS1 geometry, *i.e.* with rounded irises, we obtain $\kappa_{tot} = 601$ V/pC/m, a 3% smaller result.

We conclude that for the NLC parameters, neither the end effects, nor the tapering, nor the rounding of the irises have much effect on the wakefield. More in particular, we also conclude that the longitudinal wakefield obtained through the FD method in Ref. [2], and meant to represent the DDS1 structure, is 15% low, 8% of which is due to not having used the average cell geometry in the calculation.

4 REFERENCES

[1] "Zeroth-Order Design Report for the Next Linear Collider," SLAC Report 474 (1996).

[2] K. Bane, SLAC-NLC-Note 9, February 1995.

[3] E. Keil, *Nucl. Instr. Meth.* **100**, 419 (1972); D. Brandt and B. Zotter, CERN-ISR/TH/82-13 and LEP Note 388 (1982).

[4] S. Heifets and S. Kheifets, *Phys. Rev. D* **39**, 960 (1989).

[5] R. Gluckstern, *Phys. Rev. D* **39**, 960 (1989).

[6] K. Bane and P. Wilson, Proceedings of the 11th Int. Conf. on High Energy Accelerators, CERN (Birkhäuser Verlag, Basel, 1980), p. 592.

[7] K. Yokoya, KEK Report 90-21, September 1990, p. 142-150.

[8] A. Novokhatskii and A. Mosnier, DAPNIA-SEA-96-08, November 1996.

[9] K. Yokoya, unpublished result.

[10] G. Stupakov, Proc. of IEEE Part. Accel. Conf., Dallas, 1995, p. 3303.

[11] A. Novokhatskii and A. Mosnier, "Wakefield Dynamics in Quasi-Periodic Structures," PAC97, Vancouver, 1997.

[12] K. Bane, *et al*, DESY-M-97-02, January 1997.